JOURNAL OF AGRICULTURAL AND FOOD CHEMISTRY

Article

pubs.acs.org/JAFC

Regulation of Both the Reactive Oxygen Species Level and Antioxidant Enzyme Activity in Drought-Stressed Rice Organs by Benzimidazolate-Based SOD1 Mimics

Xianggao Meng, Min Wang, Nuowei Jiang, Dan Zhang, Li Wang, and Changlin Liu*

Key Laboratory of Pesticide and Chemical Biology, Ministry of Education, and School of Chemistry, Central China Normal University, Wuhan 430079, People's Republic of China

Supporting Information

ABSTRACT: In the study, three benzimidazolate-based Cu^{2+} complexes were identified as SOD1 mimics to explore their effects on the levels of reactive oxygen species (ROS) and activities of antioxidant enzymes in drought-stressed rice organs. Superoxide dismutase (SOD) activity of the mimics was found to be controlled by unsaturated coordination, auxiliary ligands, and counteranions. In comparison to the control, SOD1 mimic treatment for rice seeds significantly reduced ROS ($O_2^{\bullet -}$, H_2O_2, and •OH) levels in the rice leaf and root while notably increased activities of antioxidant enzymes, including SOD1 and catalase. It can enhance the tolerance of plant organs to drought stress and, thus, has a practical potency of application in rice production on arid land.

KEYWORDS: *SOD1 mimics, ROS, antioxidant enzymes, rice, drought stress*

INTRODUCTION

Superoxide dismutases (SODs) are endogenous and first-line-defense enzymes that contain either Cu/Zn, Fe, Mn, or Ni at the active site and eliminate $O_2^{\bullet -}$ by catalyzing their dismutation into O_2 and H_2O_2 with high efficiency.[1] The cytoplasmic Cu/ZnSOD enzyme (SOD1) has been shown to possess high catalytic rates of $\sim 10^9$ M^{-1} s^{-1}.[2] Each subunit in SOD1 contains an imidazolate anion-bridged Cu/Zn binding site, in which the copper ion has a distorted square pyramidal N_4O_w coordination sphere.[3] Because the metal binding site is essential for SOD activity, a large number of mononuclear Cu^{II} and dinuclear Cu^{II}/Cu^{II} or Cu^{II}/Zn^{II} complexes have been designed as SOD1 mimics to emulate the structure and function of the metal binding site.[4−18] Following the pioneering work performed by Lippard and co-workers[5−8] and recent work on the imidazolate-bridged Cu^{II}/Zn^{II} and Cu^{II}/Cu^{II} dinuclear mimics,[9−18] detailed studies on these SOD1 mimics have provided valuable insights into the structure and function of the SOD1 active site. As a result of the strong catalytic roles of the aquo Cu^{II} ion in superoxide dismutation with a catalytic rate of $\sim 10^5$ M^{-1} s^{-1}, as well as the essential concerns of toxicity that need to be considered in the use of Cu complexes as a metal-based drug, the functional study of SOD1 mimics can become a complicated process.[2,19] Therefore, the development of functional SOD enzyme mimics currently focuses mainly on the therapeutic use of Mn complexes.[19,20] However, the benzimidazolate-based SOD1 mimics have been found to be capable of enhancing the adaptability of plants to tolerate stresses.[21−25]

Reactive oxygen species (ROS) at the homeostasis level are emerging as important regulators of plant development.[26,27] Plants respond to abiotic (e.g., drought) and biotic stresses by transient increases in ROS production.[28] When the increase in the ROS production is relatively small, the housekeeping antioxidant capacity is sufficient to restore the original balance between ROS production and scavenging, thus, re-establishing redox homeostasis. At high levels (oxidative stress), ROS can behave as highly reactive and harmful species. Their superior ability to react with most cellular components provokes, among others, destructive protein modification, in addition to mutagenic DNA strand breaks, purine oxidation, and protein−DNA cross-links.[29] Eventually, high levels of ROS can lead to plant death. Drought, which is a significant limiting factor in achieving high rice production, causes serious oxidative stress, following a robust increase in ROS production in rice organs. Obviously, the efficient pathways to improve the tolerance of rice toward drought include reducing ROS production and/or increasing antioxidant enzyme activity in rice organs. In the present study, the effects of SOD1 mimics on both ROS levels and antioxidant enzyme activity in drought-stressed rice organs are explored through characterization of three simple benzimidazolate-based Cu^{2+} complexes as SOD1 mimics. The treatment of rice seeds with the SOD1 mimics was found to be capable of significantly reducing the relative ROS levels; meanwhile, a pronounced increase in activity of the antioxidant enzymes, including SOD1 and catalase (CAT), was observed in the rice leaf and root when compared to the rice organs that stemmed from the untreated seeds.

MATERIALS AND METHODS

Preparation and Characterization of the Cu^{II}−Bis-(benzimidazol-2-ylmethyl)amine (idb) Complexes 1−3. The ligand idb was synthesized according to previously reported methods.[14] The Cu^{II}−idb complexes **1**−**3** were prepared according to the following procedure: idb (0.27 g, 1.0 mmol) was mixed with

Received: May 3, 2012
Revised: October 21, 2012
Accepted: October 21, 2012
Published: October 23, 2012

$CuCl_2{\cdot}2H_2O$ (0.17 g, 1.0 mmol), $Cu(NO_3)_2{\cdot}2H_2O$ (0.24 g, 1.0 mmol), or $Cu(ClO_4)_2{\cdot}6H_2O$ (0.55 g, 1.2 mmol) in methanol (30 mL). The blue solution was stirred at 50−60 °C for 4−6 h and then allowed to dry at room temperature without disturbing. After 1 week, the blue crystals formed were filtered and washed with methanol and diethyl ether and dried *in vacuo*. Yield ∼ 70%. Suitable crystals were selected for X-ray diffraction at room temperature for complexes **1** and **3** and at low temperature (223 K) for complex **2**. X-ray diffraction and structure refinement of the Cu^{II}−idb complex **1** were described in the previously reported work,[30] and complexes **2** and **3** were described in the Supporting Information [Cambridge Crystallographic Data Centre (CCDC) reference number 889565 for complex **2** and CCDC reference number 889566 for complex **3**].

SOD Activity Assay of the Complexes 1−3. SOD activity of the Cu^{II}−idb complexes **1**−**3** was assayed by measuring the inhibition of the reaction of the water-soluble nitroblue tetrazolium salt, 2-(4-iodophenyl)-3-(4-nitrophenyl)-5-(2,4-disulfo-phenyl)-2*H*-tetrazolium monosodium salt (tetrazolium, NBT, Sigma). In the reaction, a water-soluble formazan dye was produced upon reduction with a superoxide anion. The superoxide anion is generated by the hypoxanthine−xanthine oxidase reaction. Bovine SOD1 (Sigma) was used to generate a standard curve.

Rice Materials, Growth, and Drought-Stressed Conditions. Seeds of rice (*Oryza sativa* var. Jingyou 928) were germinated in distilled water solutions of the SOD1 mimics **1**, **2**, and **3** (0, 2, 20, and 200 μM) for 3 days at 25 °C in the dark. In contrast, the same seeds were also germinated in the distilled water containing 20 μM $CuCl_2{\cdot}2H_2O$, $Cu(NO_3)_2{\cdot}2H_2O$, $Cu(ClO_4)_2{\cdot}6H_2O$, or idb under the conditions tested. Following the treatment, they were planted in pots (3 seeds/pot), containing vermiculite moistened with distilled water, and then allowed to grow in a growth chamber for 7 days. The environmental conditions in the growth chamber were 60−80% humidity, 28/25 °C for day/night temperatures, and a 16 h photoperiod with 12 000 LX of illumination. Each pot was sprinkled with 3 mL of distilled water at 22:00 each day to moisten the vermiculite. For the exposure to the drought stress, the plants were grown for 3 days without distilled water sprinkled, following growth of 7 days. Finally, root and leaf were harvested after the drought stress treatment, frozen in liquid nitrogen, and stored at −80 °C for further analysis. Untreated plants, which were germinated in the distilled water for 3 days with no Cu^{II} complexes, salts, or ligand added, grew for 7 days and were exposed to the drought stress for 3 days without distilled water sprinkled, under the same conditions. Untreated organs were harvested at the same time. All of the experiments were repeated 3 times. All experimental materials for assays were prepared using distilled water that had been passed through a Millipore-Q ultrapurification system.

Spectrophotometric Assay of Relative ROS Levels in Drought-Stressed Rice Organs. The relative $O_2^{\bullet -}$ level in the drought-stressed rice root was determined with hydroxylamine hydrochloride.[31] Briefly, the roots (0.10 g) of the treated and untreated rice samples were soaked and thoroughly homogenized in 2 mL of 10 mM phosphate-buffered saline (PBS) [phosphate buffer at pH 7.8 with 0.1 mM ethylenediaminetetraacetic acid (EDTA)]. Then, the hydroxylamine hydrochloride (10 mM, 1 mL) was added to the mixtures. Following incubation of 40 min at 37 °C, 2 mL of aminobenzene sulfonic acid (19 mM) and α-naphthlamine (7 mM) was added to the mixtures sequentially. The absorbance of the mixtures was determined at 528 nm after 10 min of incubation at 37 °C on an analytic jena SPECORD 210 spectrophotometer.

The relative H_2O_2 level in the drought-stressed rice leaf was determined according to the reported method,[32] with modification. Briefly, the rice leaf (0.15 g) was homogenized in iced trichloroacetic acid (5 mL) and centrifuged twice at 10000*g* for 20 min at 0 °C. Then, 2 mL of the supernatant, and 5 mL of KI (1.0 M) aqueous solution were transferred into PBS solution (2 mL) successively. Following 30 min of incubation at 0 °C, the absorbance of solution at 340 nm was determined with the spectrophotometer.

The relative •OH level in the rice root was determined by the terephthalic acid method.[33] Briefly, 0.050 g of rice root was homogenized with 5 mL of terephthalic acid and reacted for 40 min at 37 °C. The final solution was filtered, and the fluorescence intensity of the filtrate was determined at 426 nm with the excited wavelength of 315 nm on a Cary Eclipse spectrofluorometer.

***In Situ* Histochemical Monitoring of ROS Production in Drought-Stressed Rice Organs.** *In situ* histochemical monitoring of $O_2^{\bullet -}$ production in the leaves was performed with NBT.[34] The selected fragments (10 mm in length) of rice leaves were first soaked for 4−16 h in the PBS containing NBT (0.05%) and NaN_3 (10 mM) at 37 °C. Then, these leaves were transferred into ethanol solution and incubated for 30 min at 70 °C until blue spots appeared on them. The chlorophyll in the leaves was removed using ethanol washings 4−5 times. Lastly, the obtained leaves were examined under a Leica DMI3000B inverted fluorescence microscope. *In situ* histochemical monitoring of H_2O_2 production in the rice seedling organs was carried out with dichlorofluorescein (H_2DCFDA)[35] and diaminobenzidine (DAB).[36] The selected fragments (10 mm in length) of roots were washed 3 times with 10 mM Tris-HCl buffer (pH 7.2) and soaked in the buffer (10 mL) containing 50 mM KCl, to which 100 μL H_2DCFDA (50 mM) was added and reacted for 15 min in the dark. Then, the root fragments were washed with the buffer to remove the probe on their surfaces. These leaves and root fragments were immediately observed under a Leica TCS SP5 confocal laser scanning microscope (excited at 488 nm) and the Leica DMI4000B inverted fluorescence microscope (excitement under blue light at 450−490 nm). To perform DAB analysis, the selected leave fragments (10 mm in length) were treated as below: (i) soaked in 10 mM Tris-HCl buffer (pH 6.5) containing DAB (1 mg/mL) and incubated for 16 h at 37 °C, (ii) incubated for 30 min at 70 °C to remove the chlorophyll in the leaves, and (iii) observed under the inverted fluorescence microscope.

Assay of Activity of Antioxidant Enzymes in Drought-Stressed Rice Organs. The activity of antioxidant enzymes was assayed with spectrophotometric, native polyacrylamide gel electrophoresis (PAGE), and enzyme-linked immunosorbent assay (ELISA) methods. The crude enzymic extract was obtained as listed below: the fresh leaves (1.016 g) were homogenized with 7.5 mL of 100 mM PBS [pH 7.8 with 0.1 mM EDTA, 1% (w/v) polyvinylpyrrolidone (PVP), and 0.5% (v/v) Triton-X-100] for SOD, CAT, and glutathione reductase (GR) activity assay or 50 mM PBS (pH 7.0 with 1 mM EDTA and 5 mM ascorbate) for ascorbate peroxidase (APX) activity assays. The supernatant was obtained after centrifugation for 20 min twice at 10000*g* and 0 °C and stored at −20 °C for further analysis.

Spectrophotometric Assay.[37] Total SOD activity was assayed using a modified NBT method. Briefly, the reaction mixture (3 mL) containing 0.1 mL of enzyme extract, 0.3 mL of 7.5 mM NBT, 0.3 mL of 20 μM riboflavin, 0.3 mL of 0.13 M methionine, and 0.3 mL of 100 μM EDTA−Na_2 in 50 mM PBS (pH 7.8) was illuminated for 20 min in a box lined with aluminum foil at 25 °C. The absorbance at 560 nm of the mixture was measured immediately after the reaction was stopped. The mixture without the enzyme extract was considered as the control. To determine the CAT activity, the decomposition of H_2O_2 was monitored as a decrease in absorbance at 240 nm in the ultraviolet−visible (UV−vis) spectrophotometer. The assay mixture (3 mL) contained 2 μL of the enzyme extract in 50 mM PBS (pH 7.0) and 10 mM H_2O_2. APX activity was determined from the decrease in absorbance at 290 nm because of oxidation of ascorbate in the reaction. The 3 mL assay mixture contained 50 mM PBS (pH 7.0), 0.5 mM ascorbate, 0.5 mM H_2O_2, and 10 μL of the enzyme extract. H_2O_2 was added finally to initiate the reaction, and the decrease in absorbance was determined for 3 min using the UV−vis spectrophotometer. To determine GR activity, the increase in absorbance at 412 nm was measured when 5,5′-dithio-bis(2-nitrobenzoic acid) (DTNB) was reduced to 2-nitro-5-thiobenzoic acid (TNB) by glutathione (GSH) in the reaction. The enzyme extract (10 μL) was used in the assay along with 0.75 mM DTNB, 0.1 mM nicotinamide−adenine dinucleotide phosphate (NADPH), and 1 mM oxidized glutathione (GSSG) in a total volume of 3 mL. GSSG was added to initiate the reaction, and the increase in absorbance was determined following incubation of 3 min.

Native PAGE Assay. Activity of antioxidant enzymes was detected by zymography, following nondenaturing, nonreducing electrophoresis. SOD activity was visualized as inhibition of NBT reduction. Briefly, the gels (10% for isolation and 3.75% for concentration) were obtained following electrophoresis of the enzyme extract (15 μL) containing total SOD enzymes. Then, they were stained by sequentially soaking in 2.45 mM NTB solution in the dark for 20 min, in PBS (36 mM, pH 7.8) containing 28 μM riboflavin and 28 mM *N*,*N*,*N*′,*N*′-tetramethylethylene diamine (TEMED) in the dark for 15 min, and in 50 mM PBS (pH 7.8) with illumination for 30 min in a box lined with aluminum foil. To evaluate the SOD1 activity, the chloroform/ethanol (3:5, v/v) mixture that can inhibit MnSOD was added to the enzyme extract, and the enzyme extract was incubated at 37 °C for 20 min prior to electrophoresis. The CAT-containing gels (8% for isolation and 3% for concentration) were stained by sequentially soaking in 50 mM PBS (pH 7.0) containing 50 μg/mL horseradish peroxidase (HRP) in the dark for 45 min, in 50 mM PBS (pH 7.0) containing 5 mM H_2O_2 in the dark for 10 min, and in 50 mM PBS (pH 7.0) containing 0.5 mg/mL DAB for 4 min after washing twice. The APX-containing gels (10% for isolation and 5% for concentration) were stained by soaking in 50 mM PBS (pH 7.0) containing 4 mM ascorbate and 2 mM H_2O_2 for 45 min and by shaking for 5 min in 50 mM PBS (pH 7.8) containing 28 mM TEMED and 2.45 mM NBT, following washing twice with PBS (pH 7.0). The GR-containing gels (10% for isolation and 5% for concentration) were stained in the 0.25 M Tris-HCl buffer (pH 7.8) containing 0.24 mM 3-(4,5-dimethylthiazol-2-yl)-2,5-diphenyltetrazolium bromide (MTT), 0.4 mM NADPH, 3.6 mM GSSG, and 0.34 mM 2,6-dichlorophenolindophenol (DCPIP) in the dark for 1 h.

ELISA. The ELISA experiments of both total SOD and CAT activities were performed using a Biotek Synergy 2 multidetection microplate reader according to the instructions of the manufacturer of plant SOD and CAT ELISA kits (Rapidbio), respectively.

Statistical Analysis. GraphPad Prism software (version 4.0) was used for all statistical analysis. Data are presented as the mean ± standard deviation (SD). Data were analyzed by unpaired, two-tailed *t* tests when comparing two variables.

RESULTS AND DISCUSSION

Structure-Dependent SOD Activity of the Cu^{II}–idb Complexes. The ligand used in the preparation was idb, which contains two benzimidazolyl groups. The Cu^{II}–idb complexes **1**–**3**, which were prepared by a simple procedure, displayed subtle differences in their structure because of the use of different Cu^{II} salts (Figure 1). The complex **1**, $Cu(idb)Cl_2$, produced by the reaction of idb with $CuCl_2{\cdot}2H_2O$, had a five-coordinated trigonal–bipyramidal structure.[30] However, the reactions with either $Cu(NO_3)_2{\cdot}2H_2O$ or $Cu(ClO_4)_2{\cdot}6H_2O$ formed the square pyramid- and planar square-coordinated complexes $[Cu(idb)H_2O](NO_3)_2$ (**2**) and $[Cu(idb)H_2O]$-$(ClO_4)_2{\cdot}H_2O$ (**3**), respectively. Their donor sets of the coordination spheres around Cu^{II} centers are completed by three nitrogen atoms from idb and one or two oxygen atoms from water or anions. It is noteworthy that in the structures of complexes **2** and **3**, one coordinated water molecule and weak coordinated counter-anions [e.g., ClO_4^- in the distal of Cu^{II} in complex **3** with Cu–O bond lengths larger than 2.47(2) Å] could exert observable influences on the coordination structures of Cu^{II} ions in complexes **2** and **3**, as indicated by the structural data listed in Table S1 of the Supporting Information.

The SOD activity of complexes **1**–**3** was compared by the well-used NBT assay. The wild-type bovine SOD1 was used as a control. The results demonstrated that (i) the IC_{50} values (50% inhibitory concentrations of the SOD1 mimics) of complexes **1**–**3** were ∼2 orders of magnitude higher than that of the native enzyme and (ii) the SOD activity of complexes **1**–**3** was ∼2 orders of magnitude lower than that of the native enzyme (Table 1),[2,19] indicating that the Cu^{II} complexes can significantly catalyze the $O_2^{\bullet -}$ dismutation into O_2 and H_2O_2. In addition, the reaction rates of NBT with $O_2^{\bullet -}$ were also compared at different concentrations of the catalysts (see Table S2 of the Supporting Information). Although these data were an indirect measure of the SOD activity of the SOD1 mimics, the rate constant in the absence of complexes **1**–**3** was indeed higher than those in the presence of complexes **1**–**3**, as previously reported for wild-type SOD1.[38] This is a clear demonstration that the SOD1 mimics exhibit a notable SOD activity. Moreover, the pronounced difference in SOD activity

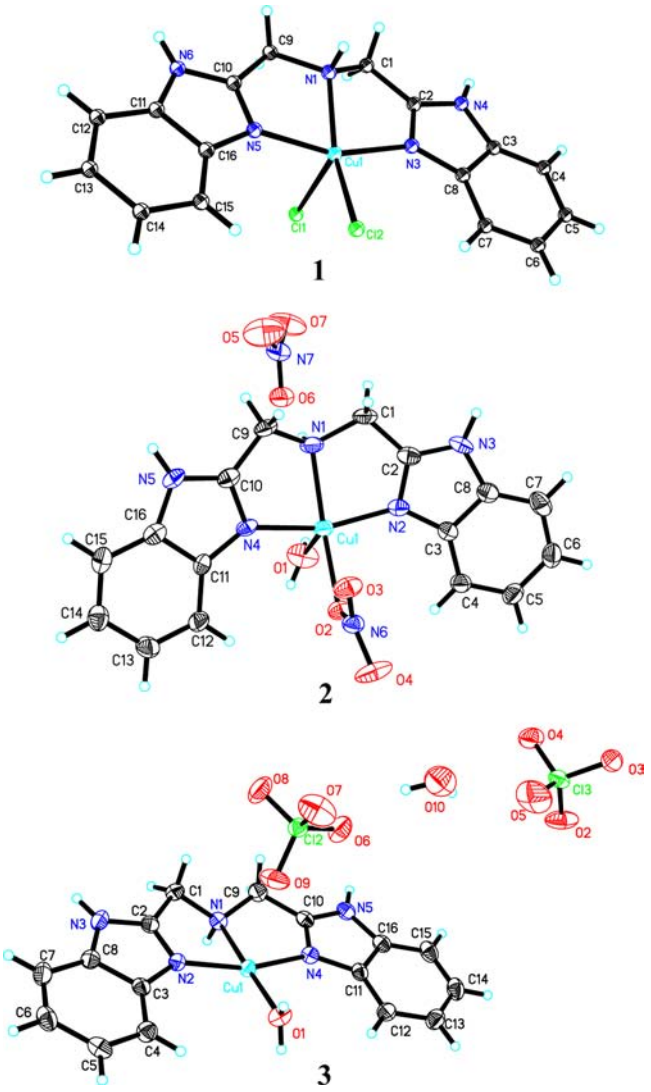

Figure 1. ORTEP view of the SOD1 mimics **1**–**3**.

Table 1. SOD Activity of the SOD1 Mimics at pH 7.8

compound	IC_{50} (μM)	SOD activity (units[a])
bovine SOD1	0.012	83333.3
1	1.18	847.5
2	1.02	980.4
3	0.84	1190.5

[a]1 unit = 1000/IC_{50} (μM^{-1}).

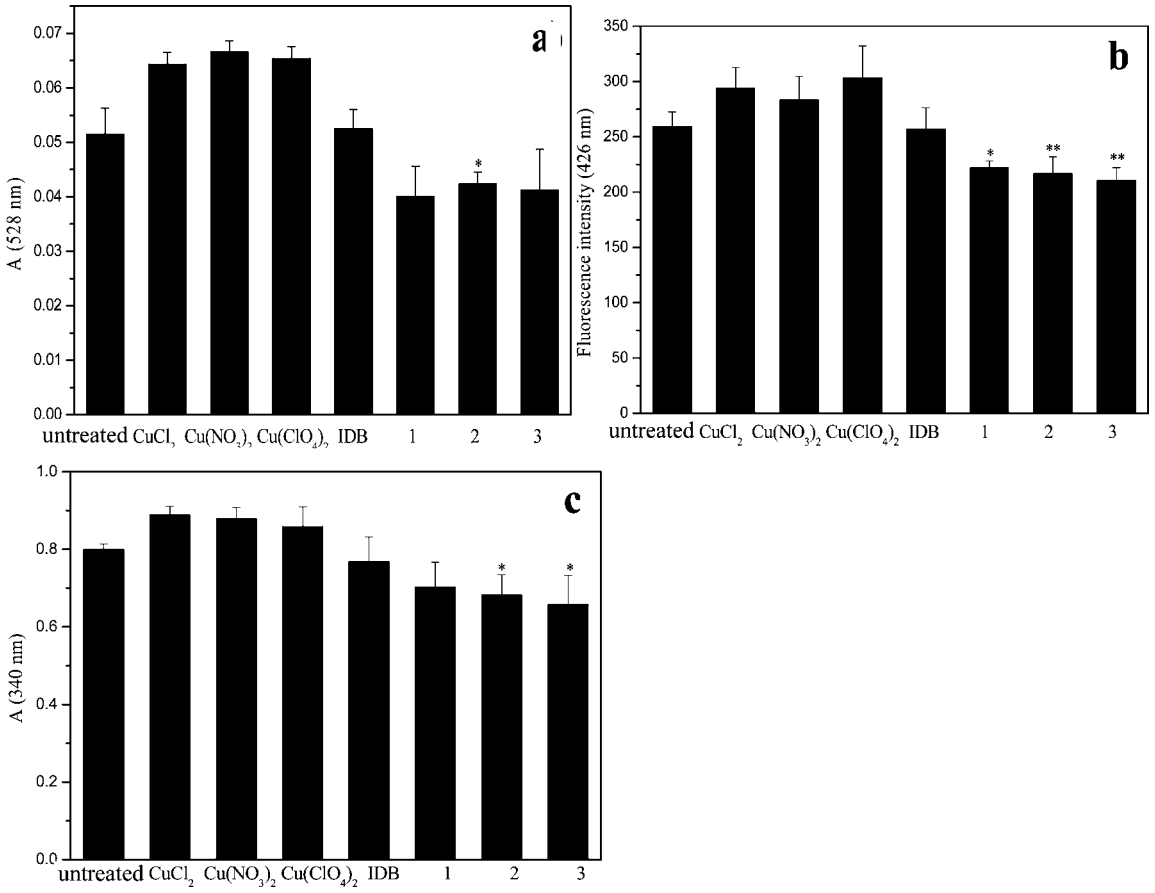

Figure 2. Spectrophotometric assays of the relative ROS levels in the (a and b) root and (c) leaf of the rice seedlings that were germinated in the solutions containing 20 μM of the SOD1 mimics, Cu^{II} salts, and idb, respectively. The absorbance at 528 or 340 nm represents the relative level of (a) $O_2^{\bullet -}$ or (c) H_2O_2, and the fluorescence intensity at 426 nm represents the relative level of (b) •OH. The unaffected organs were from the rice seeds without treatment [(**) $p < 0.01$ or (*) $p < 0.05$].

was not observed among the SOD1 mimics at the higher concentrations, but the reasons that lead to this result remain to be explored.

Evidently, the unoccupied or weak coordinated sites by the water molecule and anions around the Cu^{II} ions in the complexes are critical factors leading to the high SOD activity. This highlights the important roles of structural factors, including different auxiliary ligands (Cl^- and H_2O), low coordination numbers, and localization of different counter-anions, in SOD activity. For instance, although complex **1** has a similar structure to the Cu^{II} site in SOD1 in a sense, complexes **2** and **3** have a higher SOD activity. This might be attributed to the labile water molecule and ClO_4^- ions in complexes **2** and **3**, which are more easily replaced by other reactive oxygen anions (i.e., $O_2^{\bullet -}$ and O_2^{2-}) than Cl^- in complex **1**. The fact that complex **3** acts as a better catalyst of $O_2^{\bullet -}$ dismutation compared to complex **2** might be ascribed to the two ClO_4^- anions and one water molecule in the distal of Cu^{II}, from which three potentially activated sites can be provided. However, only two sites can be provided in complex **2** because the nitrate is more strongly coordinated to the Cu^{II} center than the perchlorate anion here [$Cu-O_{nitrate} = 2.056(3)$ Å in complex **2**, and $Cu-O_{perchlorate} = 2.466(2)$ and $2.721(2)$ Å in complex **3**]. As a result, the subtle differences in their structures lead to different SOD1 activities.

Rice Seedling Growth under the Drought-Stressed Conditions. To examine effects of the SOD1 mimics on ROS ($O_2^{\bullet -}$, H_2O_2, and •OH observed here) production in the drought-stressed rice organs, the rice seeds were first of all soaked in the solutions containing 20 μM of the SOD1 mimics, idb, and Cu^{II} salts used for preparation of the SOD1 mimics, respectively. The rice seedlings that were germinated from the untreated seeds under the environmental conditions tested (that is, the rice seeds were soaked in the distilled water with no additive) were considered as contrasts. The plants were provided only with distilled water, light, and carbon dioxide, and no nutrients were added. The growth of the rice seedlings was similar during the first 7 days, regardless of the seedlings that stemmed from the treated or untreated seeds (see panels a–d of Figure S1 of the Supporting Information). The rice seedlings, which were originated from both the untreated seeds and the seeds treated with either idb or the Cu^{II} salts, all died after the drought-stressed treatment for 3 days. However, the drought-stressed condition could not lead to death of the rice seedlings that stemmed from the seeds treated with the SOD1 mimics, although the growth of the rice seedlings was significantly stunted (see panels e and f of Figure S1 of the Supporting Information). It is notable that the growth period of the first 7 days may consume the nutrients contained in the seeds, which might considerably affect the growth of the rice seedlings.

Regulation of ROS Production in Drought-Stressed Rice Organs by the Treatment of Rice Seeds with the SOD1 Mimics. The absorbance or fluorescence intensity at the

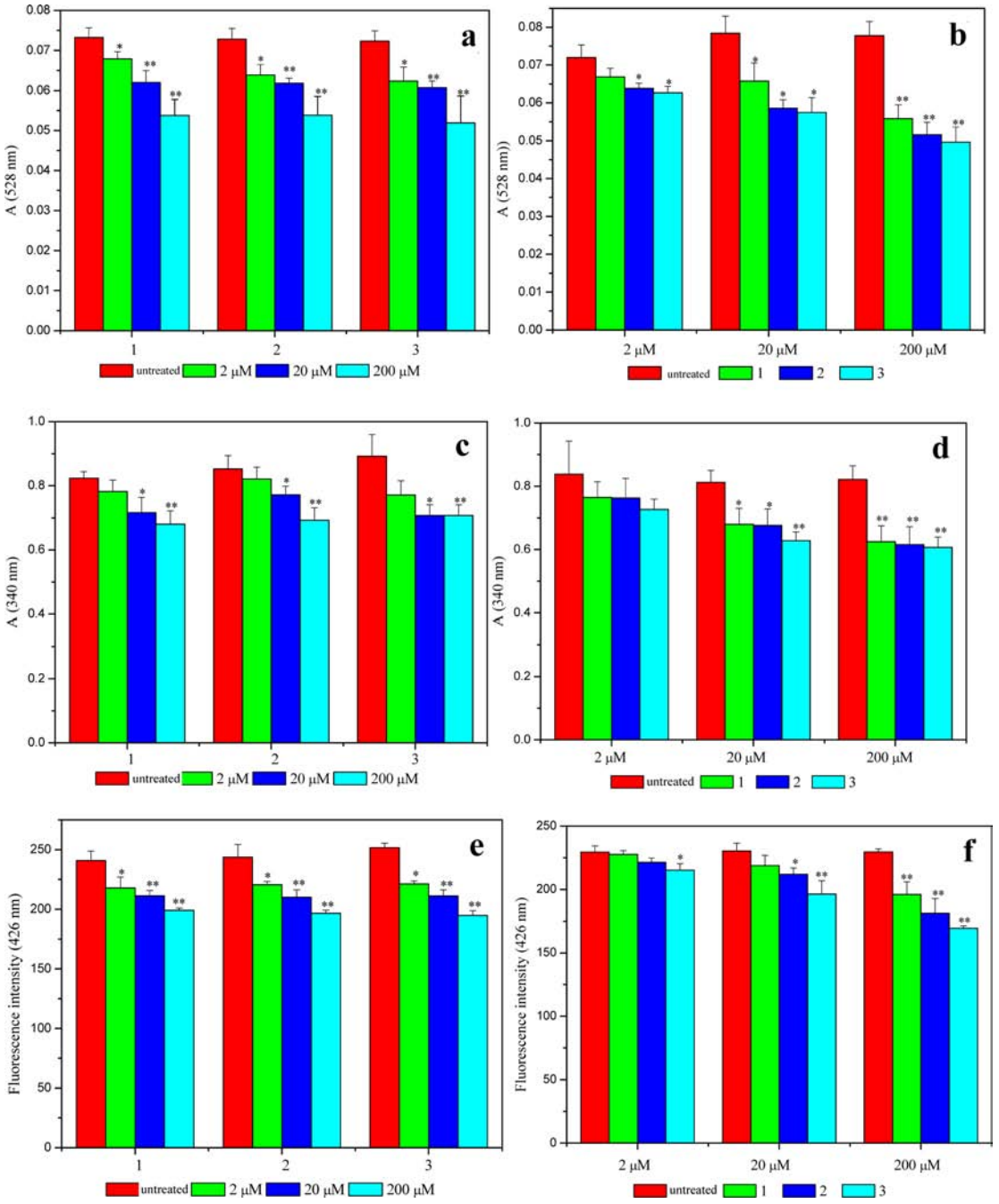

Figure 3. Spectrophotometric assays of the relative ROS levels in the (a, b, e, and f) root and (c and d) leaf of the rice seedlings that were germinated in the solutions containing the SOD1 mimics with increasing concentrations. The absorbance at 528 or 340 nm represents the relative level of (a and b) $O_2^{\bullet -}$ or (c and d) H_2O_2, and the fluorescence intensity at 426 nm represents the relative level of (e and f) •OH. The unaffected organs were from the rice seeds without treatment. [(**) $p < 0.01$ or (*) $p < 0.05$].

given wavelengths of rice materials that stemmed from the treated and untreated seeds was positively correlated with relative ROS levels. The drought stress was observed to lead to a large elevation in ROS production in the rice (see Figure S1 of the Supporting Information).[28,39] As illustrated by the spectrophotometric assays, the treatment of the rice seeds with the Cu^{II} salts led to a further increase in their relative ROS ($O_2^{\bullet -}$, H_2O_2, and •OH) levels compared to that in the rice from the untreated seeds under the drought-stressed conditions. However, the relative ROS levels in the rice organs treated with idb did remain constant compared to those in the untreated. In contrast, the relative ROS levels were significantly decreased ($p < 0.01$ or 0.05) in the rice that stemmed from the SOD1-mimic-treated seeds under the drought-stressed conditions (Figure 2). The results thus indicated that the SOD1 mimic treatment of seeds can lead to a significant reduction in ROS production.

To confirm the above-mentioned observation, the relative ROS levels were determined for the drought-stressed rice root and leaf that stemmed from the seeds exposed to the solutions containing the SOD1 mimics of varied concentrations. The absorbance or fluorescence intensity of the prepared samples at the given wavelengths (528, 340, and 426 nm) were observed to decrease with increasing concentrations of each SOD1

mimic compared to the untreated (panels a, c, and e of Figure 3). This result indicated that the relative ROS levels in the drought-stressed rice are reduced in a SOD mimic concentration-dependent manner. However, it was found that the SOD1 mimic concentrations below 2 μM had no significant effect on ROS production in the studied rice. When the SOD1 mimics were $\geq$20 μM, the ROS production was significantly reduced in the treated rice ($p < 0.05$ or 0.01) (unpublished data). Therefore, the reduction in ROS production in the rice that stemmed from the SOD1-mimic-treated seeds is SOD1-mimic-concentration-dependent.

The magnitude of reduction in the relative ROS levels in the drought-stressed rice root and leaf was compared for these three SOD1 mimics. The data indicated that complexes **2** and **3** induced a more pronounced reduction compared to complex **1** in $O_2^{\bullet -}$ production in the roots. Nonetheless, the magnitude of reduction in $O_2^{\bullet -}$ production was similar for complexes **2** and **3** (Figure 3b). The production of H_2O_2 and •OH in these organs was observed to decrease in the order of complexes **1**−**3** at the tested concentrations (panels d and f of Figure 3).

Confirmation of the Reduction in ROS Production in the Drought-Stressed Rice Organs. When plants respond to abiotic stresses, such as drought or salt, the ROS accumulation in their organs is transiently and robustly increased (see Figure S2 of the Supporting Information).[28,39] ROS accumulation in plant organs can be observed by histochemical staining with dyes or fluoresceins. The formazan formed by the reaction of NBT with $O_2^{\bullet -}$ exhibits blue spots in plant leaves after removal of chlorophyll. The number and intensity of the blue formazan spots that are observed in a unit area of leaves under an inverted microscope represent elevation or reduction in ROS production. Thus, ROS production was examined in the treated and untreated rice leaves under the drought-stressed conditions by NBT staining. The examinations verified the spectrophotometric observations that the SOD1 mimic treatment of rice seeds can significantly reduce the relative ROS levels in drought-stressed rice organs. The pictures demonstrated that the blue formazan spots were pronounced and dense in the untreated leaves (without the SOD1 mimic treatment), whereas the same area of the rice leaves that were germinated from the SOD1-mimic-treated seeds, at the given concentrations, showed significantly decreased blue spots (Figure 4a). Moreover, the number of blue spots was decreased progressively with concentrations of the SOD1 mimics. Only a few formazan spots were observed at 200 μM. In contrast, the treatment with the cupric salts led to pronouncedly increased formazan spots, and the treatment with idb did not exhibit an observable alteration in the formazan spots (see Figure S3a of the Supporting Information). These qualitative results further indicated that the $O_2^{\bullet -}$ accumulation is pronouncedly reduced in the treated leaves compared to the untreated leaves under the drought-stressed conditions.

The localization of H_2O_2 accumulation in the treated and untreated rice leaves was performed by DAB staining.[36] The reaction of DAB with H_2O_2 results in a brown product. The amount of this brown product can be conveniently assessed through examining the brown spots in the leaves under a microscope and even with naked eyes following the removal of chlorophyll. It was clearly evident that the brown spots were much smaller in the treated leaves of the same areas than those in the untreated leaves (Figure 4b). Moreover, the brown spots disappeared with doses of the SOD1 mimics. When the doses of the SOD1 mimics were 200 μM, only a few of the brown

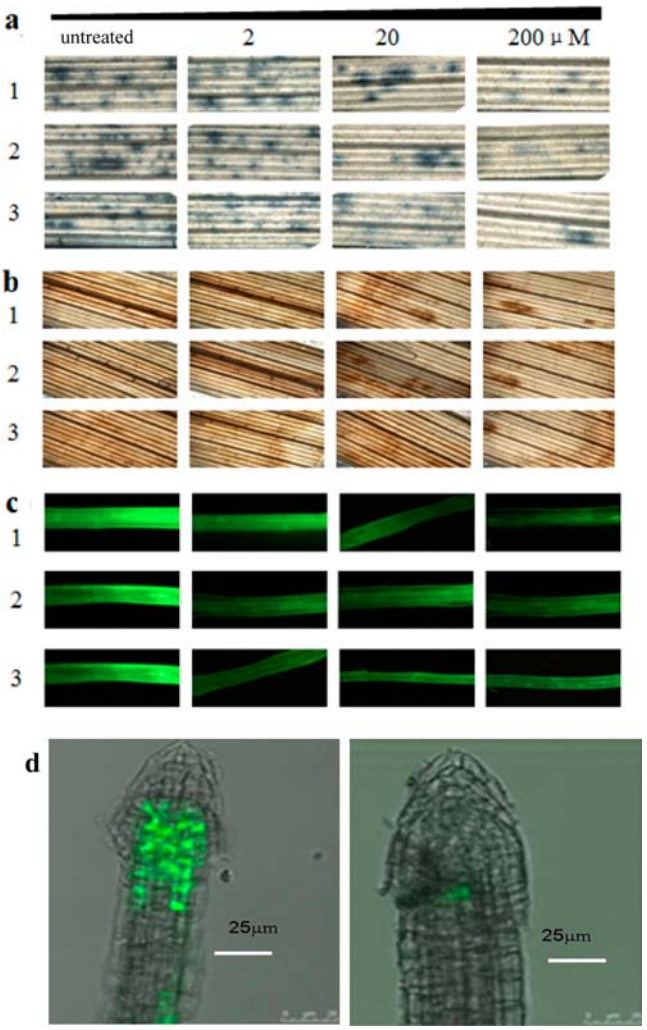

Figure 4. *In situ* histochemical monitoring of relative ROS levels in rice organs with both (a−c) an inverted fluorescence microscope and (d) a confocal laser scanning microscope. (a) Number and intensity of the blue formazan spots in an area unit of leaves represented elevation or reduction in ROS production. (b) Amount of H_2O_2 was assessed by the brown region in an area unit of leaves because the reaction of DAB with H_2O_2 generates a brown product. (c) Intensity of green fluorescence emitted by the rice roots treated with H_2DCFDA was proportional to the amount of H_2O_2 contained in the roots. (d) Accumulation of H_2O_2 was localized in the rice roots: (left) root from the untreated seeds and (right) root from the treated seeds.

spots were observed. In contrast, in comparison to the untreated leaves, the treatment with the cupric salts led to larger brown spots and the treatment with idb did not exhibit an observable alteration (see Figure S3b of the Supporting Information). The results indicated that the H_2O_2 accumulation was significantly reduced in the rice leaves that were germinated from the SOD1-mimic-treated seeds in relation to that in the leaves from the untreated seeds under the drought-stressed conditions.

The localization of H_2O_2 accumulation in the treated and untreated rice roots was examined using inverted fluorescence and confocal laser scanning microscopes. Because 2′,7′-dichlorofluorescein (DCF) is highly fluorescent, the H_2O_2-mediated oxidation of H_2DCFDA to DCF is a commonly used method to measure relative H_2O_2 levels.[35] The fluorescence microscopy pictures showed that the treated roots emitted a

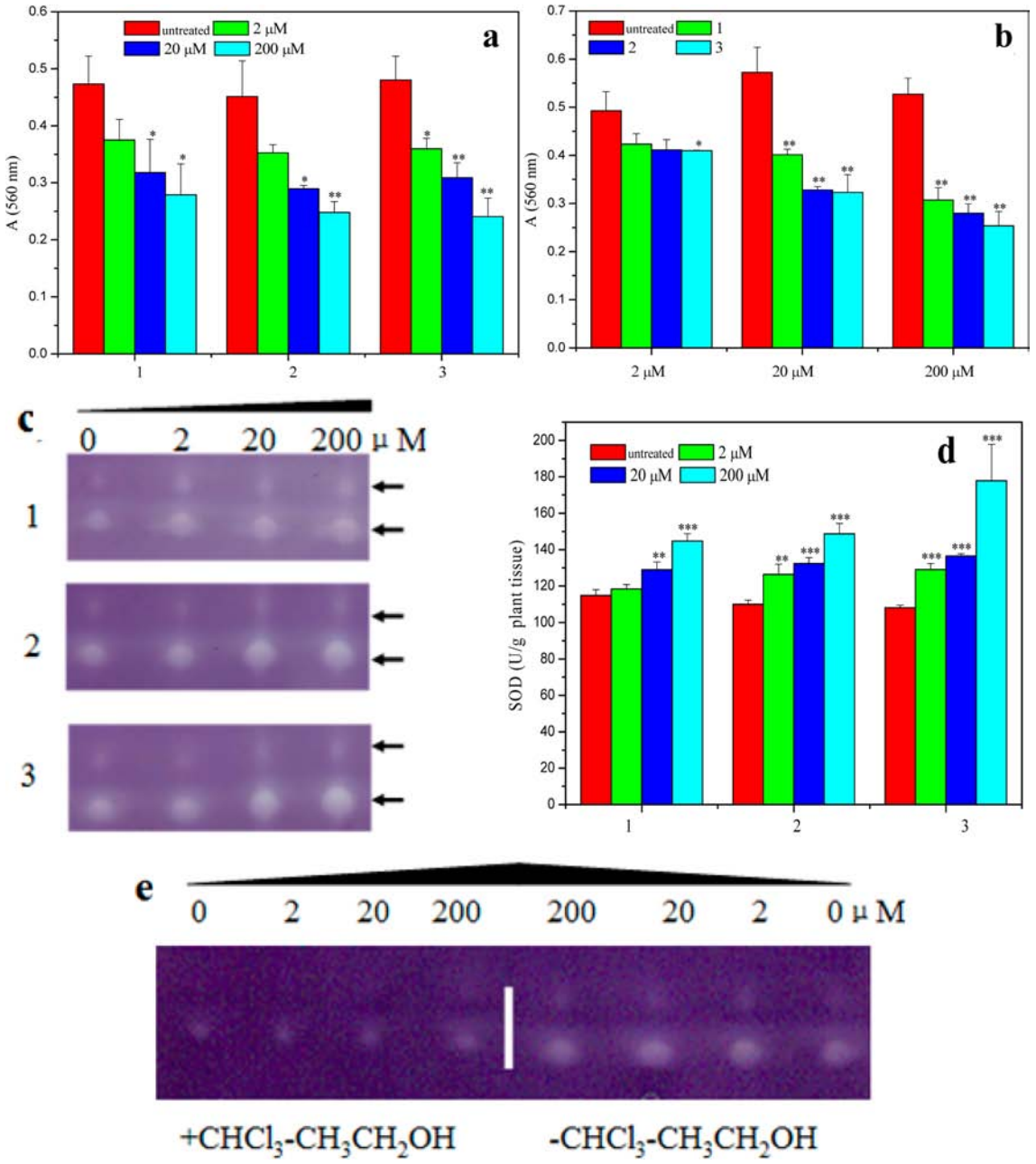

Figure 5. Assays of the total SOD and SOD1 activity in the enzyme extract from the affected and unaffected leaf. (a) Spectrophotometric assays of the SOD1 mimic dose dependence of the total SOD activity. (b) Comparison of the total SOD activity among three SOD1 mimics at the given concentrations through spectrophotometric assays. (c) Native PAGE observation of the total SOD activity in 15 μL of enzyme extract. Two SOD activity bands in the native gels, as indicated by arrows, reflected the existence of two isoforms of SOD enzymes in the enzyme extract. (d) ELISA of the total SOD activity/g of leaf was performed according to the instructions of the manufacturer of plant SOD ELISA kit. (e) Native PAGE observation of the SOD1 activity in 15 μL of enzyme extract treated with a chloroform/ethanol (3:5, v/v) mixture [(***) $p < 0.001$, (**) $p < 0.01$, or (*) $p < 0.05$].

brilliant green fluorescence. In contrast, the rice roots that were originated from the SOD1-mimic-treated seeds emitted a weak fluorescence (Figure 4c). Moreover, the green fluorescence faded away as the SOD1 mimic concentrations were increased. When the doses of SOD1 mimics were 200 μM, the fluorescence from the roots could hardly be observed. However, the treatment with the cupric salts led to an enhancement in fluorescence, and the treatment with idb led to the unchanged fluorescence (see Figure S3c of the Supporting Information). These results provided firm support to the above observation that the H_2O_2 production was significantly reduced in the plant roots from the SOD1-mimic-treated seeds compared to the plant roots from the untreated seeds under the drought-stressed conditions. This is consistent with the observation with the DAB staining that the relative H_2O_2 level was markedly reduced in the rice leaves from the SOD1-mimic-treated seeds compared to the rice leaves from the untreated seeds (Figure 4b).

In addition, the localization of H_2O_2 accumulation in the rice roots was examined also using confocal laser scanning microscopy. The brilliant green fluorescence was found to appear near the tip of the roots (left panel of Figure 4d). The

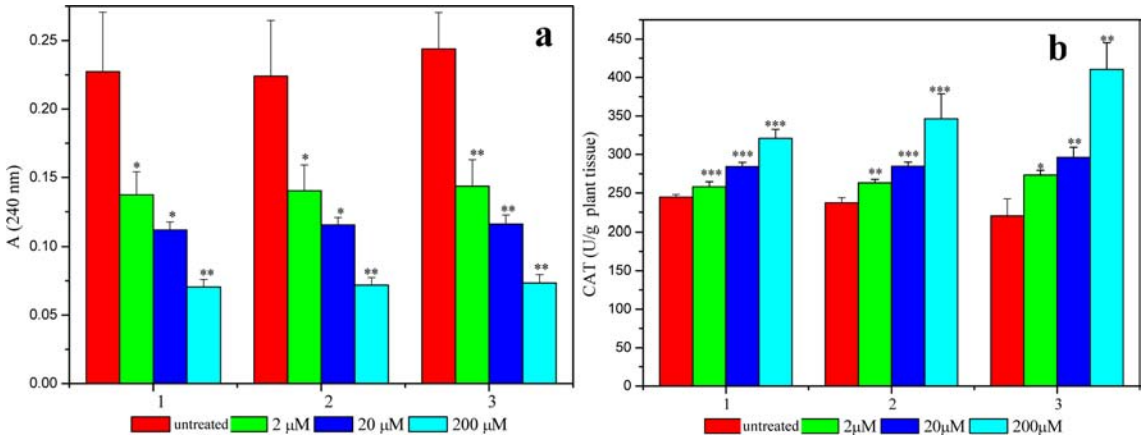

Figure 6. Assays of CAT activity in the enzyme extract from the affected and unaffected leaf. (a) Spectrophotometric assays of the SOD1 mimics dose dependence of CAT activity. (b) ELISA data of CAT activity/g of leaf were performed according to the instructions of the manufacturer of plant CAT ELISA kit [(***) $p < 0.001$, (**) $p < 0.01$, or (*) $p < 0.05$].

fluorescent spots in the untreated roots were larger and more brilliant than those in the treated roots. In fact, no apparent brilliant fluorescent spot was found in the plant roots that were originated from the seeds treated with 20 μM of the SOD1 mimics, as illustrated by the picture in right panel of Figure 4d. The results further confirmed the above observation that the SOD1 mimic treatment of the rice seeds could significantly reduce the H_2O_2 accumulation in the affected roots, which was in good agreement with the results obtained with the DAB and DCF staining.

The evidence above revealed that the relative ROS ($O_2^{\bullet -}$, H_2O_2, and •OH) levels in the drought-stressed rice organs were significantly reduced following the SOD1 mimic treatment of the seeds. The reduction of ROS production might be attributed to a potential pathway; i.e., the activity of antioxidant enzymes, including SOD1 and CAT, in the affected rice organs might be increased because of the SOD1 mimic treatment of rice seeds. This potential pathway can be explored by determining the activity of antioxidant enzymes in rice organs from treated and untreated seeds under the drought-stressed conditions through biophysical methods, including spectrophotometric assay, native PAGE, and ELISA. In addition, the possibility that SOD1 mimics might directly scavenge the excess ROS produced by the drought stress in the rice cannot be neglected, because the SOD1 mimics could enter into cells of the rice seeds through crossing both protection shells and cell walls of the rice seeds during treatment. Evidently, this needs further investigation to prove this speculation.

Enhancement of Activity of Antioxidant Enzymes in the Drought-Stressed Rice Organs by the SOD1 Mimic Treatment of Rice Seeds. Total SOD activity in 1 volume unit of the enzyme extract from the rice leaves was determined by three methods. The absorbance at 560 nm is a measure of the total SOD activity of the treated and untreated leaves in an inverse ratio; i.e., the larger the absorbance at 560 nm, the lower the total SOD activity. First, the contrasting experiments showed that not only the SOD1 mimics but also the cupric salts stimulated the SOD activity but idb did not (see Figure S4a of the Supporting Information). Then, the data from the treated leaves indicated that the absorbance at 560 nm was significantly decreased with concentrations of the SOD1 mimics relative to the untreated (Figure 5a), indicating that the total SOD activity in the rice leaves that were germinated from the treated seeds is elevated with concentrations of the SOD1 mimics. Moreover, their SOD activity was varied with types of Cu^{II}–idb mimics; the elevation mediated by complexes **2** and **3** is more pronounced than that by complex **1** (Figure 5b). The evidence firmly supporting this observation was provided by both ELISA (a plant ELISA kit from Rapidbio for the SOD activity assay) and native PAGE experiments. First, the bands in the native gels, whose intensity is a measure of the total SOD activity, became more and more pronounced with concentrations of the SOD1 mimics (Figure 5c). The contrasting observation with the cupric salts and idb provided support for this (see Figure S4b of the Supporting Information). Then, the ELISA data showed that the total SOD activity/g of leaf was elevated from ~15 activity units of the untreated to ~24 activity units with concentrations of the SOD1 mimics ($p < 0.001$; Figure 5d). Therefore, the SOD1-mimic-mediated enhancement in the total SOD activity does occur in the treated samples in comparison to the untreated. Moreover, the enhancement is SOD1-mimic-dose-dependent.

The above-observed total SOD activity might stem from both SOD1 and SOD2 (MnSOD). In fact, two SOD activity bands were evident (Figure 5c), indicating that there are two isoenzymes that contributed to the total SOD activity. However, pinpointing precisely which band reflects the antioxidant activity of SOD1 needs further exploration. Because (i) the Cu^{II} complexes were the functional mimics of SOD1 and (ii) the bold band became more pronounced with concentrations of the Cu^{II} complexes, while the weak band was maintained almost unchanged with concentrations of the Cu^{II} complexes, SOD1 could have provided the determinant contribution to the total SOD activity. Although no commercial plant SOD1 antibody for ELISA assays was available, the treatment of the enzyme extract with the chloroform/ethanol mixture prior to electrophoresis can inhibit MnSOD.[40] Therefore, only the band that reflected the SOD1 activity can be visualized in the native gels following this treatment. Figure 5e illustrated that, subsequent to the treatment, only one bold band was found in the gels, which became more and more pronounced with the concentration of the Cu^{II} complexes. Evidently, the bold band reflected the SOD1 activity because of the inhibition of MnSOD. The result suggested that (i) the contribution of SOD1 to the total activity was predominant and (ii) in comparison to the unaffected leaf, the SOD1 activity in

the affected leaf was considerably enhanced by the SOD1 mimics via a dose-dependent pathway.

CAT activity was assayed with the same methods (a plant ELISA kit from Rapidbio for CAT activity assay). The data indicated that the absorbance at 240 nm of the affected rice materials was dramatically decreased to below 50% of the unaffected with doses of the SOD1 mimics (Figure 6a). The reduction in the absorbance was a measurement of the elevation in the CAT activity. Moreover, the CAT activity was found from the ELISA data to be elevated from 33 of the untreated to 55 activity unit/g of leaf (Figure 6b). The enhancement in the CAT activity was similar to that in the total SOD activity. These two lines of evidence indicated that the CAT activity in the affected rice leaf was considerably enhanced by the SOD1 mimics via a dose-dependent pathway.

The enzyme activity of APX and GR was also evaluated by spectrophotometric and native PAGE assays. The data demonstrated that the activity of these two enzymes was markedly elevated as a result of the SOD1 mimic treatment of the rice seeds (see Figure S5 of the Supporting Information), which were indirectly corroborated by the total SOD and CAT activities.

In addition, from Figures 5 and 6 and Figure S4 of the Supporting Information, it was found that the enhancement in activity of the enzymes SOD1, CAT, and APX caused by complexes **2** and **3** was more significant than that by complex **1** at the given concentrations. This is well-consistent with the facts that the complexes **2**- and **3**-mediated reductions in ROS production were more pronounced than the complex **1**-mediated reduction (Figures 2−4). The results revealed a relation between the enhancement in activity of the antioxidant enzymes in the drought-stressed rice organs and the structures of the SOD1 mimics.

The spectrophotometric assays and *in situ* histochemical examinations indicated that the relative ROS ($O_2^{\bullet -}$, H_2O_2, and •OH) levels were significantly reduced in the affected rice leaf and root in comparison to the unaffected (Figures 2−4). The reduction in ROS production in the treated organs might be attributed to two potential pathways. The SOD activity of the SOD1 mimics could contribute to the $O_2^{\bullet -}$ clearance. Evidence for this hypothesis could be found in the higher SOD activity exhibited by complexes **2** and **3** over complex **1**, which, as a result of their more coordination-unsaturated structure, may stimulate the faster $O_2^{\bullet -}$ dismutation. The subsequent enhancement in activity of the antioxidant enzymes, including SOD1 and CAT, as proven by three lines of biophysical evidence (Figures 5 and 6 and Figure S5 of the Supporting Information), could contribute to the maintenance of ROS homeostasis in the drought-stressed rice organs. It is plausible that the organs from the rice seeds treated with complexes **2** and **3** exhibited lower ROS levels than those with complex **1**, because the treatment with complexes **2** and **3** resulted in more pronounced enhancement in activity of antioxidant enzymes in the samples than that with complex **1**. Alternatively, the reduction in ROS production, which was caused by the high SOD activity of the SOD1 mimics, the enhanced activity of the antioxidant enzymes, or both, can well be correlated with structures of the SOD1 mimics. In addition, the reduction in relative H_2O_2 and •OH levels implied that the intracellular environment may have become more reductive inside the rice cells following the SOD1 mimic treatment of the rice seeds.

The biophysical measurements all indicated that the reduction in ROS production was accompanied with the enhancement in activity of the antioxidant enzyme in the rice organs that stemmed from the SOD1-mimic-treated seeds. Consequently, this revealed that the enhanced activity of the antioxidant enzymes might be a key factor in leading to the reduction in ROS production in the drought-stressed rice that stemmed from the SOD1-mimic-treated seeds. This also provided a line of support for the hypothesis that the SOD1 mimics could maintain inside rice cells after crossing both protection shells and cell walls of the seeds. On the one hand, the intracellular SOD1 mimics might act as a source that releases copper ions to the Cu proteins and enzymes. Evidently, the copper source can be used to activate a greater amount of nascent SOD1 enzymes. However, because the coordination states of the Cu^{II} ions in the SOD1 mimics can affect the copper release, the difference in the activation degree of nascent SOD1 can be observed among the SOD1 mimics. Thus, the ligand idb in the SOD1 mimics might have behaved as an ionophore for copper. This inference is supported by the contrasting experiments, which highlighted that treatment with only idb did not exhibit any observable influence on both ROS production and antioxidant enzyme activity in the drought-stressed rice organs (Figure 2). On the other hand, the intracellular SOD1 mimics might have regulated the ROS signal transduction and, thereby, led to enhanced expression of the antioxidant enzymes, including SOD1 and CAT. Therefore, the elevation in antioxidant activity might be attributed to the additional activation of nascent Cu enzymes, including SOD1, and/or the elevated expression of the antioxidant genes in the drought-stressed rice.

The evidence presented here indicates that the SOD1 mimic treatment of rice seeds can stimulate both reduction in ROS production and enhancement in activity of the antioxidant enzymes, including SOD1, CAT, APX, and GR in the affected rice under the drought-stressed conditions. This function of the SOD1 mimics was affected by their structural factors, including coordination unsaturation and auxiliary ligands. Although the reduction in ROS production is caused by the SOD activity of the SOD1 mimics, the enhancement in activity and expression of the antioxidant enzymes, or both remains to be explored, this study indicates that the rice seeds exposed to the SOD1 mimics can enhance the resistance of plants to drought stress. It was expected that this work could expand functional uses of the metal complexes that act as the mimics of antioxidant enzymes. In addition, the SOD1-mimic-mediated improvement in drought resistance of rice, together with the best field management, might provide a pathway to maintain effective rice production.

■ ASSOCIATED CONTENT

Ⓢ Supporting Information

Additional figures and tables, as discussed in the text. This material is available free of charge via the Internet at http://pubs.acs.org.

■ AUTHOR INFORMATION

Corresponding Author

*E-mail: liuchl@mail.ccnu.edu.cn.

Funding

This work was supported by the National Science Funding of China (20971049 and 21001047) and the Program for

Changjiang Scholars and Innovative Research Team in University (PCSIRT) (IRT0953).

Notes

The authors declare no competing financial interest.

■ ABBREVIATIONS USED

APX, ascorbate peroxidase; CAT, catalase; DAB, diaminobenzidine; DCF, 2′,7′-dichlorofluorescein; DCPIP, 2,6-dichlorophenolindophenol; DTNB, 5,5′-dithio-bis(2-nitrobenzoic acid); ELISA, enzyme-linked immunosorbent assay; GR, glutathione reductase; H_2DCFDA, dichlorofluorescein; idb, bis(benzimidazol-2-ylmethyl)amine; MTT, 3-(4,5-dimethylthiazol-2-yl)-2,5-diphenyltetrazolium bromide; NBT, 2-(4-iodophenyl)-3- (4-nitrophenyl)-5-(2,4-disulfo-phenyl)-2*H*-tetrazolium; PAGE, polyacrylamide gel electrophoresis; ROS, reactive oxygen species; SOD1, Cu/Zn superoxide dismutase; SOD2, Mn superoxide dismutase; TNB, thio-2-nitro-5-thiobenzoic acid

■ REFERENCES

(1) Fridovich, I. An overview of oxyradicals in medical biology. *Adv. Mol. Cell Biol.* **1998**, *25*, 1−14.

(2) Riley, D. P. Functional mimics of superoxide dismutase enzymes as therapeutic agents. *Chem. Rev.* **1999**, *9*, 2573−2588.

(3) Tainer, J. A.; Getzoff, E. D.; Richardson, J. S.; Richardson, D. C. Structure and mechanism of copper, zinc superoxide dismutase. *Nature* **1983**, *306*, 284−287.

(4) Strothkamp, K. G.; Lippard, S. J. Chemistry of the imidazolate-bridged bimetallic center in the copper−zinc superoxide dismutase and its model compounds. *Acc. Chem. Res.* **1982**, *15*, 318−326.

(5) Kolks, G.; Frihart, C. R.; Rabinowitz, H. N.; Lippard, S. J. Imidazolate-bridged complexes of copper(II). *J. Am. Chem. Soc.* **1976**, *98*, 5720−5721.

(6) O'Young, C.-L.; Dewan, J. C.; Lilenthal, H. R.; Lippard, S. J. Electron spin resonance, magnetic, and X-ray crystallographic studies of a binuclear, imidazolate bridged copper(II) complex, $[(TMDT)_2Cu_2(im)(ClO_4)_2](ClO_4)$. *J. Am. Chem. Soc.* **1978**, *100*, 7291−7300.

(7) Coughlin, P. K.; Dewan, J. C.; Lippard, S. J.; Watanabe, E.; Lehn, J. M. Synthesis and structure of the imidazolate bridged dicopper(II) ion incorporated into a circular cryptate macrocycle. *J. Am. Chem. Soc.* **1979**, *101*, 265−266.

(8) Kolks, G.; Lippard, S. J.; Waszczak, J. V.; Lilienthal, H. R. Magnetic exchange in imidazolate-bridged copper(II) complexes. *J. Am. Chem. Soc.* **1982**, *104*, 717−725.

(9) Lu, Q.; Luo, Q. H.; Dai, A. B.; Zhou, Z. Y.; Hu, G. Z. The synthesis and crystal structure of imidazolate-bridged [Cu(tern)(im)-Zn(tren)]$(ClO_4)_3$MeOH (tren = tris(2-aminoethyl) amine; im = imidazolate]. *J. Chem. Soc., Chem. Commun.* **1990**, 1429−1430.

(10) Mao, Z.-W.; Chen, M.-Q.; Tan, X.-S.; Liu, J.; Tang, W.-X. Synthesis, crystal structure, and properties of a new imidazolate-bridged copper−zinc heterobinuclear complex with triethylenetetramine ligands. *Inorg. Chem.* **1995**, *34*, 2889−2893.

(11) Li, D. F.; Li, S.; Yang, D. X.; Yu, J. H.; Huang, J.; Li, Y. Z.; Tang, W. X. Syntheses, structures, and properties of imidazolate-bridged Cu(II)−Cu(II) and Cu(II)−Zn(II) dinuclear complexes of a single macrocyclic ligand with two hydroxyethyl pendants. *Inorg. Chem.* **2003**, *42*, 6071−6080.

(12) Pierre, J.-L.; Chautemps, P.; Refaif, S.; Beguin, C.; Marzouki, A. E.; Serratrice, G.; Saint-Aman, E.; Rey, P. Imidazolate-bridged dicopper(II) and copper-zinc complexes of a macrobicyclic ligand (cryptand). A possible model for the chemistry of Cu−Zn superoxide dismutase. *J. Am. Chem. Soc.* **1995**, *117*, 1965−1973.

(13) Ohtsu, H.; Shimazaki, Y.; Odani, A.; Yamauchi, O.; Mori, W.; Itoh, S.; Fukuzumi, S. Synthesis and characterization of imidazolate-bridged dinuclear complexes as active site models of Cu,ZnSOD. *J. Am. Chem. Soc.* **2000**, *122*, 5733−5741.

(14) Hendriks, H. M. J.; Birker, P. J. M. W. L.; Verschoor, G. C.; Reedijk, J. Dimeric copper(II) compounds with a tripodal imidazole-containing ligand and bridged by imidazolate, benzimidazolate, and benzotriazolate ions. Crystal and molecular structure of μ-(benzotriazolato-N^1,N^3)bis{[tris(N^1-methylbenzimidazol-2-ylmethyl)amine-N,N^3,$N^{3'}$,$N^{3''}$]copper(II)} trinitrate. *J. Chem. Soc., Dalton Trans.* **1982**, 623−631.

(15) Tabbi, G.; Driessen, W. L.; Reedijk, J.; Bonomo, R. P.; Veldman, N.; Spek, A. L. High SOD activity of a novel, intramolecularly imidazolato-bridged asymmetric dicopper(II) species. Design, synthesis, structure, and magnetism of copper(II) complexes with a mixed pyrazole−imidazole donor set. *Inorg. Chem.* **1997**, *36*, 1168−1175.

(16) Fu, H.; Zhou, Y. H.; Chen, W. L.; Deqing, Z. G.; Tong, M. L.; Ji, L. N.; Mao, Z. W. Complexation, structure, and superoxide dismutase activity of the imidazolate-bridged dinuclear copper moiety with β-cyclodextrin and its guanidinium-containing derivative. *J. Am. Chem. Soc.* **2006**, *128*, 4924−4925.

(17) Zhou, Y. H.; Fu, H.; Zhao, W. X.; Chen, W. L.; Su, C. Y.; Sun, H. Z.; Ji, L. N.; Mao, Z. W. Synthesis, structure, and activity of supramolecular mimics for the active site and arg141 residue of copper, zinc superoxide dismutase. *Inorg. Chem.* **2007**, *46*, 734−739.

(18) Patel, R. N.; Shukla, K. K.; Anurag, S.; Choudhary, M.; Dwivedi, S. Copper(II) complexes as superoxide dismutase mimics: Synthesis, characterization, crystal structure and bioactivity of copper(II) complexes. *Inorg. Chim. Acta* **2009**, *362*, 4891−4898.

(19) Batinić-Haberle, I.; Rebouças, J. S.; Spasojević, I. Superoxide dismutase mimics: Chemistry, pharmacology, and therapeutic potential. *Antioxid. Redox Signaling* **2010**, *13*, 877−918.

(20) Salvemini, D.; Wang, Z. Q.; Zweie, J. L.; Samouilov, A.; MacArthur, H.; Misko, T. P.; Currie, M. G.; Cuzzocrea, S.; Sikorski, J. A.; Riley, D. P. A nonpeptidyl mimic of superoxide dismutase with therapeutic activity in rats. *Science* **1999**, *286*, 304−306.

(21) Liao, Z. R.; Liu, W. Q.; Liu, J.; Jiang, Y. Q.; Shi, J.; Liu, C. A study on superoxide dismutase activity of some SOD1 model compounds. *J. Inorg. Biochem.* **1994**, *55*, 165−174.

(22) Liao, Z. R.; Shi, J.; Liu, C. A new kind of model compounds mimic multicopper enzymes. *Acta Chim. Sin.* **1995**, *53*, 147−151 (in Chinese).

(23) Xu, W.; Fu, H.; Tian, Y.; Li, J. Mechanistic study on the effect of the SOD mimics on the cold resistance of rice seedings. *J. Cent. China Norm. Univ., Nat. Sci.* **2000**, *34*, 81−83 (in Chinese).

(24) Fu, H.; Tian, Y.; Liao, Z.; Shi, J. Effects of the SOD mimics on the cold resistance of rice seedings. *Sci. Agric. Sin.* **1995**, *28*, 99−103 (in Chinese).

(25) Wang, Y.; Fu, H.; Tian, Y.; Xu, W. Effects of the SOD mimics on the cold resistance of rape seedings. *J. Cent. China Norm. Univ., Nat. Sci.* **1997**, *31*, 460−463 (in Chinese).

(26) Gapper, C.; Dolan, L. Control of plant development by reactive oxygen species. *Plant Physiol.* **2006**, *141*, 341−345.

(27) Tsukagoshi, H.; Busch, W.; Benfey, P. Transcritional regulation of ROS controls transition from proliferation to differentiation in the root. *Cell* **2010**, *143*, 606−616.

(28) Ramamurthy, M.; Nina, F. Stress response, cell death and signalling: The many faces of reactive oxygen species. *Plant Physiol.* **2003**, *119*, 56−68.

(29) Van Breusegem, F.; Dat, J. F. Reactive oxygen species in plant cell death. *Plant Physiol.* **2006**, *141*, 384−390.

(30) Meng, X.; Liu, L.; Zhou, C.; Wang, L.; Liu, C. Dinuclear copper(II) complexes of a polybenzimidazole ligand: Their structures and inductive roles in DNA condensation. *Inorg. Chem.* **2008**, *47*, 6572−6574.

(31) Elstner, E. F.; Heupel, A. Inhibition of nitrite formation from hydroxylammoniumchloride: A simple assay for superoxide dismutase. *Anal. Biochem.* **1976**, *70*, 616−620.

(32) Freinbicher, W.; Bianchi, L.; Colivicchi, M. A.; Ballini, C; Tipton, K. F.; Liner, W.; Corte, L. D. The detection of hydroxyl radicals *in vivo*. *J. Inorg. Biochem.* **2008**, *102*, 1329−1333.

(33) Sergiev, I.; Alexieva, V.; Karanov, E. Effect of spermine, atrazine and combination between them on some endogenous protective

systems and stress markers in plants. *C. R. Acad. Bulg. Sci.* **1997**, *51*, 121−124.
(34) Rossetti, S.; Bonatti, P. M. *In situ* histochemical monitoring of ozone- and TMV-induced reactive oxygen species in tobacco leaves. *Plant Physiol. Biochem.* **2001**, *39*, 433−442.
(35) Zhang, H.; Xia, Y.; Wang, G.; Shen, Z. Excess copper induces accumulation of hydrogen peroxide and increases lipid peroxidation and total activity of copper−zinc superoxide dismutase in roots of *Elsholtzia haichowensis*. *Planta* **2008**, *227*, 465−475.
(36) Hu, X.; Jiang, M.; Zhang, A.; Lu, J. Abscisic acid-induced apoplastic H_2O_2 accumulation up-regulates the activities of chloroplastic and cytosolic antioxidant enzymes in maize leaves. *Planta* **2005**, *223*, 57−68.
(37) Elavarthi, S.; Martin, B. Spectrophotometric assays for antioxidant enzymes in plants. In *Plant Stress Tolerance, Methods in Molecular Biology*; Sunkar, R., Ed.; Springer Science + Business Media, LLC: Berlin, Germany, 2010; Vol. *639*, Chapter 16.
(38) Beyer, W.; Fridovich, I. Assaying for superoxide dismutase activity: Some large consequences of minor changes in conditions. *Anal. Biochem.* **1987**, *161*, 559−566.
(39) Pitzschke, A.; Hirt, H. Mitogen-activated protein kinases and reactive oxygen species signaling in plants. *Plant Physiol.* **2006**, *141*, 351−356.
(40) Gueta-Dahan, Y.; Yaniv, Z.; Zilinskas, B. A.; Ben-Hayyim, G. Salt and oxidative stress: Similar and specific responses and their relation to salt tolerance in *Citrus*. *Planta* **1997**, *203*, 460−469.